# Vertical Macular Asymmetry Measures Derived From SD-OCT for Detection of Early Glaucoma

Farideh Sharifipour,[1,2] Esteban Morales,[1] Ji Woong Lee,[1,3] JoAnn Giaconi,[1] Abdelmonem A. Afifi,[4] Fei Yu,[1,4] Joseph Caprioli,[1] and Kouros Nouri-Mahdavi[1]

[1]Glaucoma Division, Stein Eye Institute, David Geffen School of Medicine, University of California Los Angeles, California, United States
[2]Department of Ophthalmology, Ahvaz Jundishapur University of Medical Sciences, Ahvaz, Iran
[3]Department of Ophthalmology, Pusan National University College of Medicine, Busan, South Korea
[4]Department of Biostatistics, Jonathan and Karin Fielding School of Public Health, University of California Los Angeles, Los Angeles, California, United States

Correspondence: Kouros Nouri-Mahdavi, Stein Eye Institute, 100 Stein Plaza, Los Angeles, CA 90095, USA;
nouri-mahdavi@jsei.ucla.edu.

Submitted: March 29, 2017
Accepted: June 22, 2017

Citation: Sharifipour F, Morales E, Lee JW, et al. Vertical macular asymmetry measures derived from SD-OCT for detection of early glaucoma. *Invest Ophthalmol Vis Sci*. 2017;58:4030–4037. DOI:10.1167/iovs.17-21961

**Purpose.** To test the hypothesis that vertical asymmetry in macular ganglion cell/inner plexiform layer (GCIPL) thickness can improve detection of early glaucoma.

**Methods.** Sixty-nine normal eyes and 101 glaucoma eyes had macular imaging with spectral-domain optical coherence tomography (OCT; 200 × 200 cube). The resulting GCIPL thickness matrix was grouped into a 20 × 20 superpixel array and superior superpixels were compared to their inferior counterparts. A global asymmetry index (AI) was defined as the grand mean of the asymmetry ratios. To measure local asymmetry, the corresponding thickness measurements of three rows above and below the horizontal raphe were compared individually and in combinations. Global and local AIs were compared to the best-performing GCIPL thickness parameters with area under the receiver operating curves (AUC) and sensitivity/specificities.

**Results.** Age or axial length did not influence AIs in normal subjects ($P \geq 0.08$). Global and local AIs were significantly higher in the glaucoma group compared to normal eyes. Minimum (AUC = 0.962, 95% confidence interval [CI]: 0.936–0.989) and inferotemporal thickness (AUC = 0.944, 95% CI: 0.910–0.977; $P = 0.122$) performed best for detection of early glaucoma. The AUC for global AI was 0.851 (95% CI: 0.792–0.909) compared to 0.916 (95% CI: 0.874–0.958) for the best local AI. Combining minimum or inferotemporal GCIPL thickness and the best local AI led to higher partial AUCs (0.088 and 0.085, 90% specificity, $P = 0.120$ and 0.130, respectively) than GCIPL thickness measures.

**Conclusions.** Macular vertical thickness asymmetry measures did not perform better than sectoral or minimum GCIPL thickness for detection of early glaucoma. Combining local asymmetry parameters with the best sectoral GCIPL thickness measures enhanced this task.

Keywords: optical coherence tomography, early glaucoma, vertical macular thickness asymmetry, asymmetry index, ganglion cell/inner plexiform layer

Glaucoma is characterized by progressive loss of retinal ganglion cells and their axons. There is a large body of evidence suggesting that structural changes can be detected several years before measurable visual loss.[1–8] Improvements in the resolution of OCT has enabled us to measure thickness of retinal layers with a precision of 3 to 6 μm.[9] Performance of regional macular ganglion cell/inner plexiform layer (GCIPL) thickness measurements is comparable to that of peripapillary retinal nerve fiber layer (ppRNFL) thickness for the detection of early glaucoma.[10–12]

Early attenuation of retinal nerve fiber layer or GCIPL thinning in glaucoma is usually greater on one side of the horizontal meridian, most frequently inferiorly.[13] The asymmetry between threshold sensitivities of superior and inferior hemifields on standard automated perimetry is the basis for the glaucoma hemifield test (GHT)[14] used for detection of early glaucomatous field loss. Several studies have evaluated if the vertical asymmetry in full macular or GCIPL thicknesses measured by OCT can serve as a biomarker for early glaucoma.[15–23] Most have used OCT posterior pole asymmetry analysis (PPAA; Spectralis; Heidelberg Engineering, Dossenheim, Germany) program or global or local measures of vertical asymmetry and showed significant vertical asymmetry in glaucoma patients compared to normal individuals.[17–22]

The goal of the current study was to test the hypothesis that biomarkers of vertical macular thickness asymmetry based on GCIPL measurements can improve discrimination of early perimetric glaucoma from normal subjects.

## Materials and Methods

We recruited normal subjects and glaucoma patients from ongoing studies at Stein Eye Institute that were all approved by the institutional review board at the University of California Los Angeles (UCLA). This cross-sectional case-control study adhered

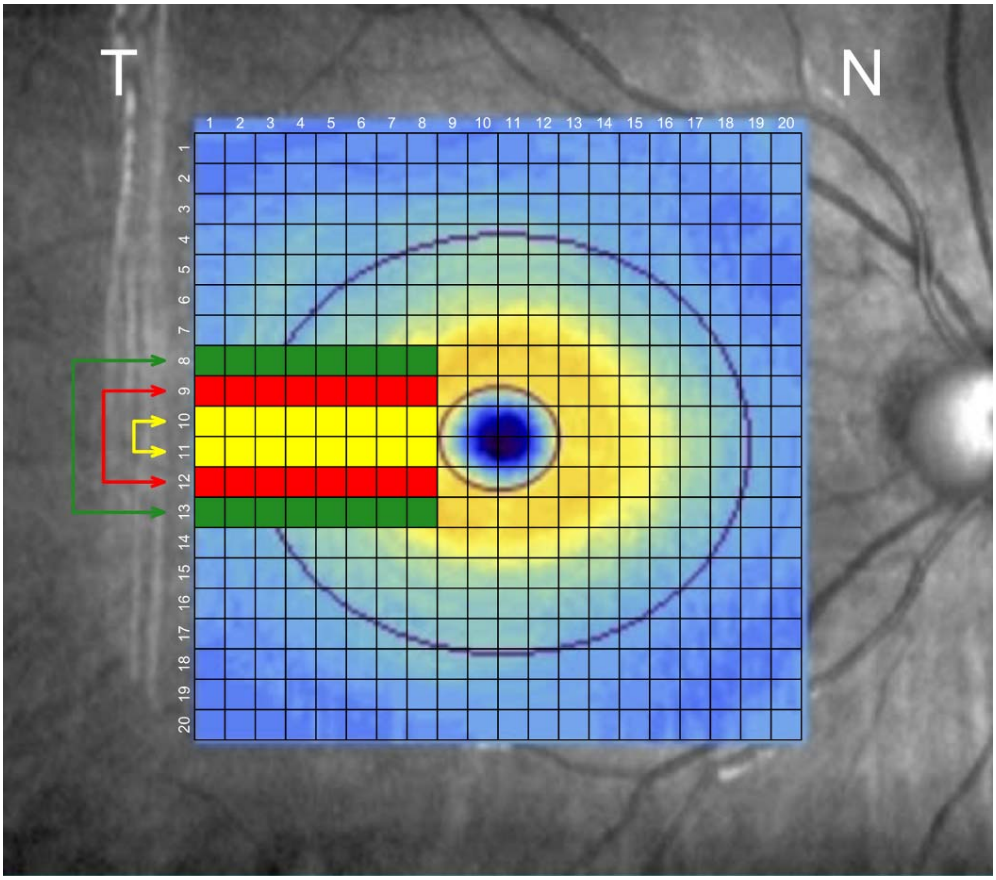


**Figure 1.** The 200 × 200 macular cube (Carl Zeiss Meditec, Inc.) consists of 40,000 A-scan measurements that were clustered into a 20 × 20 grid of superpixels centered on the fovea. Local asymmetry measures were defined based on comparison of the GCIPL thickness on the three corresponding pairs of rows above and below the temporal horizontal raphe including four or eight temporal columns, both individually and in combination. The best performing local asymmetry parameter was the one incorporating the three rows above and below the temporal raphe consisting of eight superpixels.

to the tenets of Declaration of Helsinki. Patients with open-angle glaucoma were enrolled in the study if they met the following criteria: age ≥30 years; open angles; visual acuity equal or better than 20/80; refractive error less than 8.0 diopters (D); and astigmatism ≤3 D. Clinical diagnosis of glaucoma was initially made by a glaucoma specialist at Stein Eye Institute's Glaucoma Division based on the presence of characteristic optic nerve head changes detected on slit lamp funduscopy and/or 3-D disc photographs, presence of RNFL defects on dilated funduscopy, and/or characteristic visual field defects on SAP. The enrolled eyes were later confirmed to have changes consistent with glaucomatous optic neuropathy on review of stereoscopic disc photographs; all eyes had evidence of early glaucomatous field loss (see below). Eyes with evidence of retinal or neurologic diseases were excluded. Normal subjects were recruited by advertising on UCLA's campus-wide website, placing fliers in the clinics, and soliciting spouses and friends of patients examined at the Stein Eye Institute's Glaucoma Clinic. The enrolled normal subjects were required to have open angles, corrected visual acuity of 20/25 or better, normal eye examination, normal visual fields, and lacked definitive evidence of glaucomatous damage at the level of the optic nerve head on review of stereoscopic optic disc photographs by two clinicians (KNM, JAG).

All subjects underwent a thorough eye examination on the day of imaging, including visual acuity, automated refraction, measurement of intraocular pressure (IOP); gonioscopy; slit-lamp exam; dilated fundus exam; and standard achromatic perimetry (SAP). Axial length and keratometry were measured with an optical biometer (IOLMaster; Carl Zeiss Meditec, Inc., Jena, Germany). Stereoscopic disc photographs and 200 × 200 macular cubes (Cirrus high-definition [HD]-OCT; Carl Zeiss Meditec, Inc.) were obtained after pupillary dilation. All the images were reviewed afterward by one of the investigators, and images with signal strength <7, obvious motion artifact, or incorrect segmentation were excluded.

A total of 69 eyes from 69 normal subjects and 101 eyes from 101 early glaucoma patients were included in the study. Eyes with visual field mean deviation (MD) equal to or better than –6 dB were considered to have early glaucoma.[24]

## Imaging Methods

The 200 × 200 macular cube (Carl Zeiss Meditec, Inc.) consists of 40,000 A-scans in a 6 × 6 mm grid (in an emmetropic eye with axial length of 24.46 mm) centered on the fovea. The raw images were exported and the macular GCIPL layers were segmented by custom software at Carl Zeiss Meditec headquarters and the GCIPL thickness measurements were provided to the investigators in 200 × 200 matrices. The data matrices were centered in relation to the foveal center. Thickness data of the left eyes were flipped to convert them to the right eye format. The 40,000 A-scan measurements were then clustered into a 20 × 20 grid of superpixels (Fig. 1), and various approaches were explored to compare the superior

Investigative Ophthalmology & Visual Science

**Table 1.** Demographic and Clinical Findings of Subjects Enrolled in the Study

| | Normal | Early Glaucoma | *P* Value |
|---|---|---|---|
| Eyes, *n* (subjects) | 69 (69) | 101* (101) | |
| Age, y (range) | 56.6 ± 10.3 (28.7 to 77.8) | 66.2 ± 8.5 (35 to 78.7) | <0.001 |
| Sex, male/female | 23/46 | 35/66 | 0.768† |
| Race, % | | | |
| Asian | 9 (13) | 11 (11) | <0.001† |
| African-American | 10 (14) | 10 (10) | |
| Hispanic | 17 (25) | 8 (8) | |
| White | 33 (48) | 70 (69) | |
| Indian-American | 0 | 2 (2) | |
| Visual acuity, logMAR (range) | 0.03 ± 0.08 (−0.1 to 0.30) | 0.02 ± 0.13 (−0.3 to 0.48) | 0.933 |
| Refractive error, D (range) | −0.4 ± 1.8 (−5.6 to 2.9) | −1.2 ± 2.3 (−7.25 to 3.6) | 0.118 |
| IOP, mm Hg‡ (range) | 14.6 ± 2.6 (9 to 21) | 14.0 ± 4.0* (4 to 29) | 0.866 |
| Central corneal thickness, μm (range) | 558 ± 37 (457 to 631) | 544 ± 38 (425 to 634) | 0.075 |
| Axial length, mm (range) | 23.8 ± 1 (21.9 to 16.1) | 24.6 ± 1.3 (21.4 to 28.8) | <0.001 |
| Mean deviation, dB (range) | −0.1 ± 1.2 (−3.9 to 2.26) | −2.9 ± 2 (−6 to 2.53) | <0.001 |
| Pattern standard deviation, dB (range) | 1.5 ± 0.3 (1 to 2.67) | 4.9 ± 2.7 (1.4 to 10.8) | <0.001 |

* Clinical diagnosis included 15 normal tension glaucoma, 5 pseudoexfoliation glaucoma, 2 pigmentary glaucoma, and 79 primary open-angle glaucoma eyes.

† Fisher's exact test.

‡ Treated IOPs on the day of imaging.

superpixels to their inferior counterparts. The global and sectoral GCIPL thickness measurements were also exported as extensible markup language files.

We used four different methods to compare each pair of superior and inferior superpixels and to obtain an asymmetry index (AI) as below:

1. superior/inferior thickness
2. |log (superior/inferior thickness)|
3. |superior-inferior thickness/max (superior, inferior)|
4. |superior- inferior thickness|

Global AI was defined as the grand mean of the asymmetry values in the central circular area (6-mm diameter).[22] To evaluate local asymmetry, we compared AIs based on three corresponding pairs of rows above and below temporal horizontal line singly and in combinations using the above-mentioned methods including eight or four superpixels on each row temporal to the fovea (Fig. 1). This area is where early glaucomatous damage commonly occurs and roughly corresponds to nasal visual field loss.[25]

### Statistical Analyses

Sidak or Mann-Whitney *U*, and $\chi^2$ tests were used for descriptive analyses and for parameter comparisons between groups. Univariate linear regression analysis was used to explore the relationship between AI and age, sex, and axial length. In addition to global asymmetry, performance of local asymmetry measures (with the aforementioned four methods) was explored comparing the three corresponding pairs of rows above and below the temporal horizontal line. Areas under the receiver operating curve (AUC) after logistic regression were estimated to compare performance of global and local asymmetry biomarkers to the best-performing GCIPL parameters for glaucoma detection. Partial AUC (pAUC) at 90% specificity was also compared between groups. All global and local asymmetry analyses used absolute values of the asymmetry indices with methods 2 through 4. For analyses using method 1, if the inferior superpixel was thinner than the corresponding superior superpixel, 1 / AI was used.

Statistical analyses were performed with the commercial software (Stata, version 12.1; StataCorp, College Station TX, USA) and R software (version 3.3.2). All analyses included took into account the difference in age between the two groups. Values of *P* less than 0.05 were considered as significant.

## Results

We enrolled 69 normal eyes (69 subjects) and 101 early glaucoma eyes (101 patients). Table 1 summarizes the demographic and clinical characteristics of the study sample. The normal group was significantly younger than the glaucoma group ($P < 0.001$). Regression analysis showed no significant relationship between global or local asymmetry measured by any method and age ($P = 0.445$ and 0.192, respectively for method 2); sex ($P = 0.652$ and 0.840 for method 2); or axial length ($P = 0.08$ and 0.08 for method 2) in normal individuals.

The glaucoma asymmetry index with method 2 (|log (superior/inferior thickness)|) performed best among all asymmetry indices and therefore, all analyses presented here used this method. The global AI was significantly higher in glaucoma group compared to normal eyes (Table 2). Among the local asymmetry methods, the index combining the three rows above versus the 3 rows below the temporal horizontal line demonstrated the best performance (Table 3). All local asymmetry methods using eight temporal superpixels in each row performed significantly better than methods including only four temporal superpixels in the analysis ($P < 0.001$).

The best-performing local GCIPL thickness parameters for detection of early glaucoma were the minimum GCIPL (AUC = 0.962, 95% confidence interval [CI]: 0.936–0.989) and inferotemporal (AUC = 0.944, 95% CI: 0.910–0.977; $P = 0.122$) for the difference between the two; Table 3). The calculated AUCs for global AIs by all four methods were significantly lower than that of local AIs and sectoral GCIPL thicknesses, ($P = 0.007$, Table 3; Fig. 2). The area under the receiver operating curve for the best local AI (i.e., the one combining 3 rows above and below the horizontal raphe) was significantly smaller than that of the minimum GCIPL ($P = 0.008$), but was not significantly different from the AUC for inferotemporal GCIPL thickness ($P = 0.158$, Table 3).

Combining inferotemporal sector and the best local AI significantly increased the diagnostic performance of infero-

**Table 2.** Comparison of Sectoral GCIPL Thicknesses and Local and Global AIs Between Study Groups

| | Normal | Early Glaucoma | *P* Value |
|---|---|---|---|
| Minimum GCIPL thickness, μm | 79.3 ± 6.4 | 55.5 ± 9.9 | <0.001 |
| Average GCIPL thickness, μm | 81.1 ± 6.5 | 65.8 ± 8.3 | <0.001 |
| Inferotemporal GCIPL thickness, μm | 81.5 ± 6.1 | 62.1 ± 9.8 | <0.001 |
| Inferonasal GCIPL thickness, μm | 80.6 ± 7.2 | 65.5 ± 10.7 | <0.001 |
| Superotemporal GCIPL thickness, μm | 80.5 ± 6.1 | 66.2 ± 11.7 | <0.001 |
| Superonasal GCIPL thickness, μm | 82.5 ± 7.1 | 70.5 ± 11 | <0.001 |
| Inferior GCIPL thickness, μm | 79.6 ± 7.1 | 61.6 ± 9.4 | <0.001 |
| Superior GCIPL thickness, μm | 81.7 ± 7.0 | 68.0 ± 11.0 | <0.001 |
| Global AI* | 0.02 ± 0.01 | 0.04 ± 0.03 | <0.001 |
| Local AI† | 0.02 ± 0.01 | 0.07 ± 0.05 | <0.001 |
| Local AI‡ | 0.02 ± 0.01 | 0.08 ± 0.05 | <0.001 |
| Local AI§ | 0.02 ± 0.01 | 0.06 ± 0.04 | <0.001 |
| Local AI‖ | 0.06 ± 0.03 | 0.20 ± 0.14 | <0.001 |

* Calculated as |log superior/inferior GCIPL thickness|.

† AI between the 3rd row above and below temporal horizontal raphe.

‡ AI between the 2nd row above and below temporal horizontal raphe.

§ AI between the 1st row above and below temporal horizontal raphe.

‖ AI between combined 3 rows above and below temporal horizontal raphe.

temporal GCIPL thickness in early glaucoma (AUC: 0.960 compared to AUC = 0.944 for inferotemporal sector, $P = 0.04$, Table 3) and improved the sensitivity of the combined parameter at 90% specificity from 71% to 93%. Adding the best local asymmetry to minimum GCIPL thickness led only to a small nonsignificant increase in the AUC from 0.962 to 0.965 ($P = 0.392$, Table 3).

Global AI also had the lowest pAUC as compared to minimum or inferotemporal GCIPL, and best local AI (pAUC = 0.024 vs. 0.085, 0.081, and 0.065, respectively, $P < 0.001$ for all pairwise differences between global AI and other parameters). A combination of minimum or inferotemporal GCIPL thickness and the best local AI had higher pAUCs (0.088 and 0.085, respectively) than all individual parameters including minimum GCIPL; however, the difference did not reach statistical significance ($P = 0.12$ and 0.13, respectively).

## Discussion

Our study showed that the performance of vertical GCIPL thickness asymmetry along the horizontal temporal line (based on various global or local criteria) was not as good as the best regional GCIPL thickness measures (minimum GCIPL or inferotemporal GCIPL sector) for detection of early glaucoma; however, combining the best-performing local asymmetry parameter with the inferotemporal sector GCIPL thickness improved performance of macular OCT measures based on AUCs. However, based on the pAUCs at ≥90% specificity cutoff (where it matters most clinically), the combination of local asymmetry and either the inferotemporal or minimal GCIPL thickness had a better ability to discriminate glaucomatous from normal eyes than either thickness measures alone although this difference did not reach statistical significance.

The advent of SD-OCT technology has resulted in significant research endeavors to help diagnose glaucoma at an earlier

**Table 3.** Values of AUC for GCIPL Thickness and Local and Global AIs

| | Minimum GCIPL thickness AUC (95% CI) | Inferotemporal GCIPL Thickness AUC (95% CI) | Local AI* AUC (95% CI) | Local AI† AUC (95% CI) | Local AI‡ AUC (95% CI) | Local AI§ AUC (95% CI) | Global AI AUC (95% CI) | Combining Best Local AI and IT GCIPL Thickness AUC (*P*)‖, (95% CI) | Combining Best Local AI and Minimum GCIPL Thickness AUC (*P*)¶, (95% CI) |
|---|---|---|---|---|---|---|---|---|---|
| Early glaucoma | 0.962 (0.936–0.989) | 0.944 (0.910–0.977) | 0.910 (0.865–0.954) | 0.909 (0.865–0.953) | 0.907 (0.863–0.951) | 0.916 (0.874–0.958) | 0.851 (0.792–0.909) | 0.960 ($P = 0.04$), (0.931–0.989) | 0.965 ($P = 0.392$), (0.939–0.992) |
| Sensitivity/Specificity, % | 96/98 | 94/81 | 44/97 | 81/84 | 81/86 | 84/83 | 57/81 | 92/94 | 93/100 |
| Cutoff value | 70 | 73 | 0.03 | 0.03 | 0.03 | 0.08 | 0.02 | | |
| Sensitivity#, % | 93 | 71 | 47 | 75 | 71 | 75 | 51 | 93 | 93 |
| Cutoff value | 71 | 79 | 0.02 | 0.04 | 0.03 | 0.10 | 0.03 | | |

* Between the 3rd row above and below temporal horizontal raphe.
† Between the 2nd row above and below temporal horizontal raphe.
‡ Between the 1st row above and below temporal horizontal raphe.
§ Between combined 3 rows above and below temporal horizontal raphe.
‖ Comparison of AUCs between inferotemporal GCIPL thickness and combined local AI and inferotemporal thickness.
¶ Comparison of AUCs between minimum GCIPL thickness and combined local AI and minimum thickness.
# Sensitivity at ≥90% specificity.

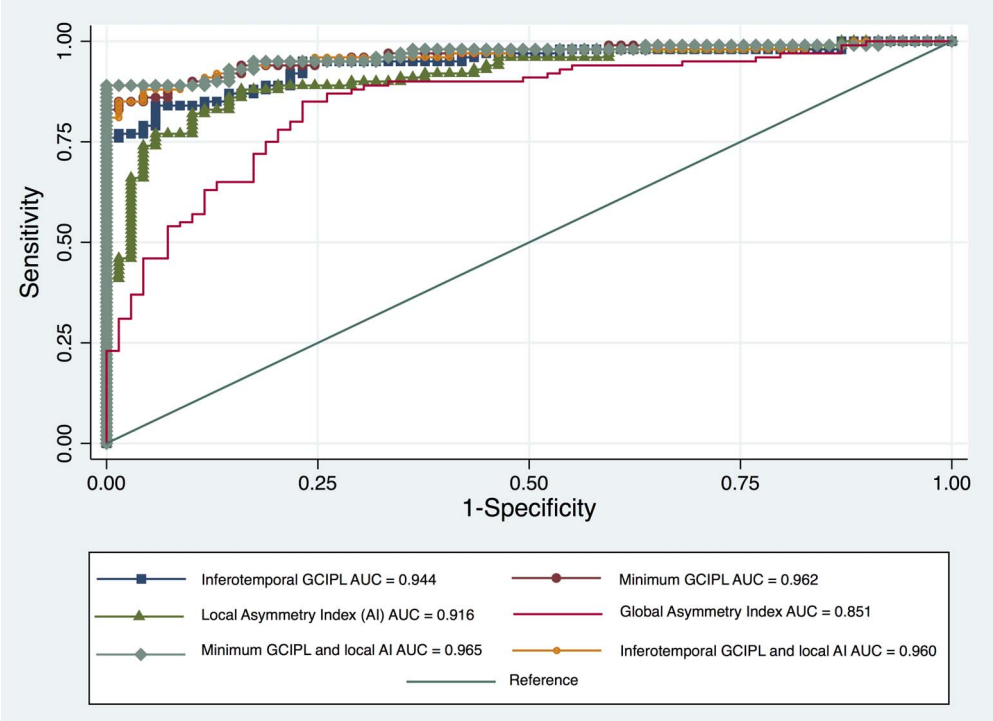


**Figure 2.** Receiver operating characteristic curves comparing glaucoma diagnostic capabilities of the best local asymmetry index, global asymmetry index, inferotemporal, and minimal GCIPL thicknesses, and combination of the best local asymmetry and regional GCIPL thickness measures.

stage before functional loss occurs. In line with this strategy, ppRNFL thickness and various inner macular thickness measurements have been used to improve glaucoma detection. Several studies have shown that measurements of inner retinal layer (IRL) thickness in localized sectors have a better diagnostic performance compared to average macular IRL or full thickness and are comparable to average ppRNFL thickness for detection of early glaucoma.[10,11,26–33]

Our study showed that regional GCIPL thickness measures outperformed global and local vertical asymmetry outcome measures. In agreement with some previous reports, our study revealed that a global asymmetry index, which is the average of all asymmetry values across the horizontal meridian, had the worst performance for discrimination of early glaucoma from normal controls.[20] Glaucoma frequently starts as a localized thinning in retinal tissue, which might go undetected by averaging asymmetry measures across the macula. Local asymmetry measures could actually detect regional changes across the temporal horizontal line and performed significantly better than global asymmetry measures in this study. Neither the global index nor local asymmetry indices were affected by age, sex, or axial length and were significantly higher in glaucoma group compared to normal individuals.

There are some reports indicating that intraeye asymmetry between superior and inferior total macular or inner layer thicknesses has equal or greater ability than ppRNFL and ganglion cell complex (GCC) measurements for detection of early glaucoma,[15–22] although the method used for estimation of asymmetry has varied among such studies. Asrani et al.[17] were the first to customize the macular thickness map of the Spectralis SD-OCT to an $8 \times 8$ grid centered on the fovea and positioned symmetrically to the fovea-disc axis. Intra- and intereye cell-to-cell comparisons were made using a cutoff value of $\geq$30 μm and the difference presented as a grayscale grid. This was later implemented as the PPAA program on Spectralis SD-OCT.[17] Seo et al.[18] showed that the diagnostic ability of PPAA for localized RNFL defects was comparable to ppRNFL thickness measurements. In a study by Um et al.[19] exploring the Spectralis posterior pole retinal thickness map, hemifield asymmetry in macular full thickness measurements was evaluated in five corresponding superior and inferior zones similar to GHT in perimetry. The macular hemifield test had significantly higher sensitivity and similar specificity compared to average ppRNFL thickness in early glaucoma, but showed comparable sensitivities and specificities in glaucoma suspects and advanced glaucoma. Diagnostic performance of the macular hemifield test was comparable to sectoral ppRNFL thickness measurements. Sullivan-Mee and colleagues[20] studied inter- and intraeye asymmetry of ppRNFL and macular thickness measurements on Spectralis PPAA for detection of early glaucoma. Intereye asymmetry parameters had the highest diagnostic sensitivities, although RNFL thickness had better overall performance than total macular thickness. Intra-eye macular thickness asymmetry had the lowest sensitivity and lowest AUC of all studied parameters. The authors reported optimal cutoff values of 5 and 9 μm for inter-eye and intra-eye macular thickness asymmetry, respectively.[20]

Yamashita and colleagues[21] demonstrated that the symmetry of retinal thickness between upper and lower cells was high in the central and temporal-macular areas but not in the peripheral and nasal macular areas with a range of difference of 3.1 to 23.2 μm. This might be due to lower reproducibility of thickness measurements temporal to the optic disc.[34] In a study of preperimetric glaucoma eyes with only inferior RNFL defects, significant asymmetry in macular thickness was reported compared to normal eyes.[35] Macular symmetry was measured as (inferior thickness/ superior thickness) ×100 on images from Topcon SD-OCT. The authors also reported significantly thinner inferior macular thickness in normal eyes.[35] Yamada et al.[22] showed that asymmetry between upper

and lower macular hemifield ganglion cell layer thickness had excellent diagnostic performance for early glaucoma compared to full thickness or inner retinal layer thicknesses in Japanese patients. They devised an asymmetry index based on 10 vertically oriented B-scans performed on the Spectralis OCT according to this formula:

$$\text{asymmetry index} = \left|\log_{10}\left(\frac{\text{lower hemiretinal thickness}}{\text{upper hemiretinal thickness}}\right)\right|.$$

Interestingly, the performance of this asymmetry index did not change with severity of glaucoma. Similarly, Kim et al.[23] reported that a local asymmetry approach utilizing differences in GCIPL thickness within 10 pixels above and below temporal horizontal raphe performed better than the best sectoral GCIPL thickness for detection of early glaucoma in a group of Korean patients. In a similar approach to our study, Hwang et al.[36] reported good diagnostic ability of asymmetry analysis in early glaucoma.

We explored various definitions of vertical asymmetry both globally and regionally and compared their diagnostic performance to each other and also to the best sectoral GCIPL thickness. Interestingly, we observed that the simple difference between superior and inferior macular thickness (which is currently in use by Spectralis PPAA) had the worst diagnostic performance among the four methods of asymmetry explored. Other methods had similar AUCs for detection of early glaucoma, although method 2 (similar to the method presented by Yamada et al.) was the best. The contradictory results reported by different studies may be explained by the limitations inherent to imaging devices. Spectralis SD-OCT provides higher resolution and possibly more precise segmentation compared to $200 \times 200$ macular cube images of Cirrus HD-OCT, but uses the fovea-disc axis as the reference line for vertical asymmetry in PPAA, as opposed to the horizontal meridian in Cirrus OCT; some investigators such as Yamada and colleagues[22] used a specific imaging protocol based on vertical lines perpendicular to the horizontal meridian. The differences in study populations in terms of ethnicity and type of glaucoma may also contribute to disagreement among studies since Asian studies include more normal-tension glaucoma (NTG).

Our study is the first to explore the performance of various global and local GCIPL-based temporal asymmetry measures in a diverse ethnic group of patients in the United States. One reason for the less optimal performance of local or global asymmetry measures in our study sample could be the lower prevalence of NTG in the US population. Only 15% of our study patients were diagnosed as NTG. Normal-tension glaucoma, which results in deep localized defects in central visual field and macular region early in the disease course,[37] could result in significant vertical asymmetry before marked retinal thickness changes are detectable. Therefore, it is possible that the performance of vertical asymmetry measures may depend on the underlying diagnosis and/or population from which the study sample originates. This may explain why Yamada et al.[22] and Kim and colleagues[23] found asymmetry measures to perform much better compared to total or inner retinal thickness measurements for glaucoma detection.

We observed that combining inferotemporal GCIPL thickness and local asymmetry measures significantly improved the diagnostic performance compared to the inferotemporal sector alone ($P = 0.04$, Table 3; Fig. 2). Despite the fact that both measures already had large AUCs, their combination led to a significant increase in glaucoma diagnostic capability similar to that of minimum GCIPL. Not every device provides the minimum GCIPL parameter and hence, combining inferotemporal inner macular thickness and local asymmetry measures would actually be an equivalent surrogate for this parameter. Additionally, when pAUCs were used to compare the performance of various thickness parameters above 90% specificity, not only did the best local vertical asymmetry measure have an equal performance to minimum GCIPL thickness, but also combining the asymmetry measures with either minimum or GCIPL thickness further enhanced performance at high specificity where it is most relevant for early detection of glaucoma—although this difference did not reach statistical significance.

One of the limitations of our study is that the macular images were not specifically designed to identify vertical asymmetry across the temporal horizontal line and hence the resolution of the images was likely less than optimal. It is possible that the performance of macular asymmetry indices will improve as customized algorithms are more widely adopted and the quality of OCT images improves. We assumed that the temporal raphe is approximately aligned with the horizontal line extending temporally from the center of the fovea. It has been shown that temporal raphe greatly varies among individuals and that the raphe-fovea-disc line looks more like a broken line with an average angle of 170°. However, currently, there is no easy way to exactly define the location of the temporal raphe on commercially available OCT images. We were able to investigate only GCIPL thickness asymmetry; however, other than the report by Yamada et al.,[22] there is no strong evidence in the literature for the superiority of the ganglion cell layer or GCC measurements to GCIPL thickness measures. In a recent study, Miraftabi and colleagues[38] found that GCIPL actually demonstrated the strongest structure-function relationship among all macular parameter with central visual fields. Our control group was significantly younger than the glaucoma group. To address this age was entered as a covariate in all models. Our study did not include angle closure glaucoma eyes. This potentially limits the generalizability of our study.

## Conclusions

Our study demonstrated that temporal vertical asymmetry in macular GCIPL thickness was comparable to sectoral inferotemporal GCIPL thickness for detection of early glaucoma although minimal GCIPL had the best nominal AUC. The performance of the global asymmetry index was worse than all local vertical asymmetry indices and the best sectoral GCIPL thickness measures. A combination of sectoral GCIPL thickness and the best local vertical asymmetry parameter significantly improved the diagnostic performance of macular images and may be implemented in OCT devices to enhance detection of early glaucoma.

### *Acknowledgments*

Presented as a poster at the annual meeting of the Association for Research in Vision and Ophthalmology, Denver, Colorado, United States, May 2015.

Supported by an National Institutes of Health Mentored Patient-oriented Research Career Development Award (5K23EY022659; KNM) and an unrestricted Departmental Grant from Research to Prevent Blindness.

Disclosure: **F. Sharifipour**, None; **E. Morales**, None; **J.W. Lee**, None; **J. Giaconi**, None; **A.A. Afifi**, None; **F. Yu**, None; **J. Caprioli**, None; **K. Nouri-Mahdavi**, Carl Zeiss Meditec (F), Heidelberg Engineering (F)

### *References*

1. Sommer A, Miller NR, Pollack I, Maumenee AE, George T. The nerve fiber layer in the diagnosis of glaucoma. *Arch Ophthalmol*. 1977;95:2149–2156.

2. Sommer A, Katz J, Quigley HA, et al. Clinically detectable nerve fiber atrophy precedes the onset of glaucomatous field loss. *Arch Ophthalmol*. 1991;109:77–83.
3. Motolko M, Drance SM. Features of the optic disc in preglaucomatous eyes. *Arch Ophthalmol*. 1981;99:1992–1994.
4. Tuulonen A, Lehtola J, Airaksinen PJ. Nerve fiber layer defects with normal visual fields. Do normal optic disc and normal visual field indicate absence of glaucomatous abnormality? *Ophthalmology*. 1993;100:587–597; discussion 597–598.
5. Kass MA, Heuer DK, Higginbotham EJ, et al. The Ocular Hypertension Treatment study: a randomized trial determines that topical ocular hypotensive medication delays or prevents the onset of primary open-angle glaucoma. *Arch Ophthalmol* 2002;120:701–713; discussion 829–830.
6. Subbiah S, Sankarnarayanan S, Thomas PA, Nelson Jesudasan CA. Comparative evaluation of optical coherence tomography in glaucomatous, ocular hypertensive and normal eyes. *Indian J Ophthalmol*. 2007;55:283–287.
7. Inuzuka H, Kawase K, Sawada A, Aoyama Y, Yamamoto T. Macular retinal thickness in glaucoma with superior or inferior visual hemifield defects. *J Glaucoma*. 2013;22:60–64.
8. Kuang TM, Zhang C, Zangwill LM, Weinreb RN, Medeiros FA. Estimating lead time gained by optical coherence tomography in detecting glaucoma before development of visual field defects. *Ophthalmology*. 2015;122:2002–2009.
9. Sung KR, Kim JS, Wollstein G, Folio L, Kook MS, Schuman JS. Imaging of the retinal nerve fibre layer with spectral domain optical coherence tomography for glaucoma diagnosis. *Br J Ophthalmol*. 2011;95:909–914.
10. Mwanza JC, Durbin MK, Budenz DL, et al. Glaucoma diagnostic accuracy of ganglion cell-inner plexiform layer thickness: comparison with nerve fiber layer and optic nerve head. *Ophthalmology*. 2012;119:1151–1158.
11. Rolle T, Briamonte C, Curto D, Grignolo FM. Ganglion cell complex and retinal nerve fiber layer measured by Fourier-domain optical coherence tomography for early detection of structural damage in patients with preperimetric glaucoma. *Clin Ophthalmol*. 2011;5:961–969.
12. Nouri-Mahdavi K, Nowroozizadeh S, Nassiri N, et al. Macular ganglion cell/inner plexiform layer measurements by spectral domain optical coherence tomography for detection of early glaucoma and comparison to retinal nerve fiber layer measurements. *Am J Ophthalmol*. 2013;156:1297–1307.e2.
13. Hood DC, Raza AS, de Moraes CG, Liebmann JM, Ritch R. Glaucomatous damage of the macula. *Prog Retin Eye Res*. 2013;32:1–21.
14. Sommer A, Duggan C, Auer C, Abbey H. Analytic approaches to the interpretation of automated threshold perimetric data for the diagnosis of early glaucoma. *Trans Am Ophthalmol Soc*. 1985;83:250–267.
15. Bagga H, Greenfield DS, Knighton RW. Macular symmetry testing for glaucoma detection. *J Glaucoma*. 2005;14:358–363.
16. Salgarello T, Colotto A, Valente P, et al. Posterior pole retinal thickness in ocular hypertension and glaucoma: early changes detected by hemispheric asymmetries. *J Glaucoma*. 2005;14:375–383.
17. Asrani S, Rosdahl JA, Allingham RR. Novel software strategy for glaucoma diagnosis: asymmetry analysis of retinal thickness. *Arch Ophthalmol*. 2011;129:1205–1211.
18. Seo JH, Kim TW, Weinreb RN, Park KH, Kim SH, Kim DM. Detection of localized retinal nerve fiber layer defects with posterior pole asymmetry analysis of spectral domain optical coherence tomography. *Invest Ophthalmol Vis Sci*. 2012;53:4347–4353.
19. Um TW, Sung KR, Wollstein G, Yun SC, Na JH, Schuman JS. Asymmetry in hemifield macular thickness as an early indicator of glaucomatous change. *Invest Ophthalmol Vis Sci*. 2012;53:1139–1144.
20. Sullivan-Mee M, Ruegg CC, Pensyl D, Halverson K, Qualls C. Diagnostic precision of retinal nerve fiber layer and macular thickness asymmetry parameters for identifying early primary open-angle glaucoma. *Am J Ophthalmol*. 2013;156:567–577.e1.
21. Yamashita T, Sakamoto T, Kakiuchi N, Tanaka M, Kii Y, Nakao K. Posterior pole asymmetry analyses of retinal thickness of upper and lower sectors and their association with peak retinal nerve fiber layer thickness in healthy young eyes. *Invest Ophthalmol Vis Sci*. 2014;55:5673–5678.
22. Yamada H, Hangai M, Nakano N, et al. Asymmetry analysis of macular inner retinal layers for glaucoma diagnosis. *Am J Ophthalmol*. 2014;158:1318–1329.e3.
23. Kim YK, Yoo BW, Kim HC, Park KH. Automated detection of hemifield difference across horizontal raphe on ganglion cell–inner plexiform layer thickness map. *Ophthalmology*. 2015;122:2252–2260.
24. Hodapp E PRI, Anderson DR. Hodapp E, Parrish RK II, Anderson DR. *Clinical Decisions in Glaucoma*. St Louis, MO: The CV Mosby Co. 1993:52–61.
25. Nascimento VC, Kasahara N, Cohen R, Almeida GV, Mandia C, Paolera MD. Location and frequency of visual field defects as measured by SITA (Swedish Interactive Threshold Algorithm) strategy in primary open angle glaucoma [in Portuguese]. *Arq Bras Oftalmol*. 2005;68:661–665.
26. Kotera Y, Hangai M, Hirose F, Mori S, Yoshimura N. Three-dimensional imaging of macular inner structures in glaucoma by using spectral-domain optical coherence tomography. *Invest Ophthalmol Vis Sci*. 2011;52:1412–1421.
27. Takayama K, Hangai M, Durbin M, et al. A novel method to detect local ganglion cell loss in early glaucoma using spectral-domain optical coherence tomography. *Invest Ophthalmol Vis Sci*. 2012;53:6904–6913.
28. Tan O, Chopra V, Lu AT, et al. Detection of macular ganglion cell loss in glaucoma by Fourier-domain optical coherence tomography. *Ophthalmology*. 2009;116:2305–2314.e2.
29. Kim NR, Lee ES, Seong GJ, Kim JH, An HG, Kim CY. Structure-function relationship and diagnostic value of macular ganglion cell complex measurement using Fourier-domain OCT in glaucoma. *Invest Ophthalmol Vis Sci*. 2010;51:4646–4651.
30. Seong M, Sung KR, Choi EH, et al. Macular and peripapillary retinal nerve fiber layer measurements by spectral domain optical coherence tomography in normal-tension glaucoma. *Invest Ophthalmol Vis Sci*. 2010;51:1446–1452.
31. Mori S, Hangai M, Sakamoto A, Yoshimura N. Spectral-domain optical coherence tomography measurement of macular volume for diagnosing glaucoma. *J Glaucoma*. 2010;19:528–534.
32. Hirashima T, Hangai M, Nukada M, et al. Frequency-doubling technology and retinal measurements with spectral-domain optical coherence tomography in preperimetric glaucoma. *Graefes Arch Clin Exp Ophthalmol*. 2013;251:129–137.
33. Lisboa R, Paranhos A, Weinreb RN, Zangwill LM, Leite MT, Medeiros FA. Comparison of different spectral domain OCT scanning protocols for diagnosing preperimetric glaucoma. *Invest Ophthalmol Vis Sci*. 2013;54:3417–3425.
34. Miraftabi A, Amini N, Gornbein J, et al. Local variability of macular thickness measurements with sd-oct and influencing factors. *Trans Vis Sci Tech*. 2016;5(4):5.
35. Kawaguchi C, Nakatani Y, Ohkubo S, Higashide T, Kawaguchi I, Sugiyama K. Structural and functional assessment by hemispheric asymmetry testing of the macular region in


Investigative Ophthalmology & Visual Science

preperimetric glaucoma. *Jpn J Ophthalmol*. 2014;58:197–204.

36. Hwang YH, Ahn SI, Ko SJ. Diagnostic ability of macular ganglion cell asymmetry for glaucoma. *Clin Exp Ophthalmol*. 2015;43:720–726.
37. Thonginnetra O, Greenstein VC, Chu D, Liebmann JM, Ritch R, Hood DC. Normal versus high tension glaucoma: a comparison of functional and structural defects. *J Glaucoma* 2010;19:151–157.
38. Miraftabi A, Amini N, Morales E, et al. Macular SD-OCT outcome measures: comparison of local structure-function relationships and dynamic range. *Invest Ophthalmol Vis Sci*. 2016;57:4815–4823.

Investigative Ophthalmology & Visual Science